

Understanding Class Bias Amplification in Graph Representation Learning

Shengzhong Zhang

*College of Computer Science and Technology
Nanjing University of Aeronautics and Astronautics*

szzhang@nuaa.edu.cn

Wenjie Yang*

School of Data Science, Fudan University

yangwj24@m.fudan.edu.cn

Yimin Zhang

School of Data Science, Fudan University

yiminzhang20@fudan.edu.cn

Hongwei Zhang

School of Data Science, Fudan University

zhanghw.hongwei@gmail.com

Zengfeng Huang*

*School of Data Science, Fudan University
Shanghai Innovation Institution*

huangzf@fudan.edu.cn

Reviewed on OpenReview: <https://openreview.net/forum?id=SqpgDUDRE9>

Abstract

Recent research reveals that GNN-based graph representation learning may inadvertently introduce various structural biases. In this work, we discover a phenomenon of structural bias in graph representation learning called class bias amplification, which refers to the exacerbation of performance bias between different classes by GNN encoder. We conduct an in-depth theoretical study of this phenomenon from a novel spectral perspective. Our analysis suggests that structural disparities between nodes in different classes result in varying local convergence speeds for node embeddings. This phenomenon leads to bias amplification in the classification results of downstream tasks. Based on the theoretical insights, we propose random graph coarsening, which is proved to be effective in dealing with the above issue. Finally, we propose an unsupervised graph contrastive learning model called Random Graph Coarsening Contrastive Learning (RGCCCL), which utilizes random coarsening as data augmentation and mitigates class bias amplification by contrasting the coarsened graph with the original graph. Extensive experiments on various datasets demonstrate the advantage of our method when dealing with class bias amplification.

1 Introduction

Graph representation learning (GRL) aims to generate embedding vectors capturing both the structure and feature information. Graph neural networks (GNNs) are the primary encoder architecture for GRL (Bojchevski & Günnemann, 2018; Zhu et al., 2020; 2021; Zhang et al., 2021; Zheng et al., 2022; Yang et al., 2026), which are often trained with unsupervised graph contrastive objectives. Such methods are called graph contrastive learning (GCL) and exhibit outstanding performance in various downstream tasks. Compared to traditional unsupervised GRL methods (Perozzi et al., 2014; Grover & Leskovec, 2016), the distinctiveness of GCL lies in the GNN encoder’s use of message passing. Due to the encoder’s use of message passing, the final embeddings are likely to inherit the structural bias in the graph, which may cause undesirable performance

*Corresponding authors.

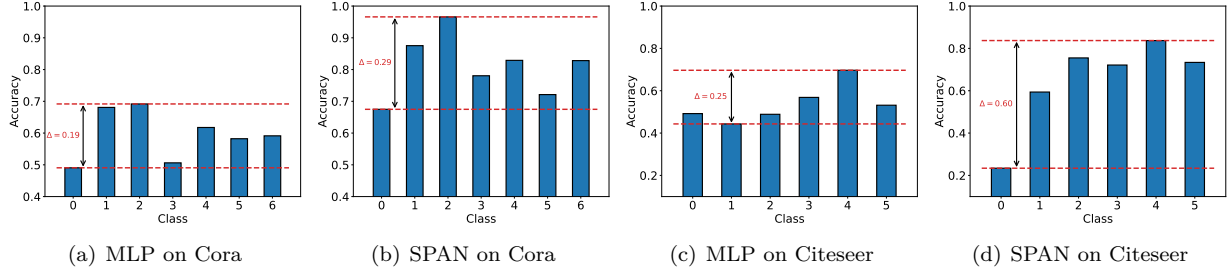


Figure 1: The classification performance of MLP and SPAN in different classes on Cora and Citeseer, where each class has 20 labeled nodes in the training set. Δ represents the maximum performance difference observed between classes.

unfairness in downstream tasks. This phenomenon is demonstrated in Figure 1, where we compare the node classification performance of MLP (utilizing feature information only) and the state-of-the-art GCL model SPAN (Lin et al., 2023). Although SPAN has a much better overall accuracy than MLP, SPAN exhibits greater performance differences between different classes of nodes. In other words, GNN-based GRL exacerbates the performance bias between different classes.

We refer to the phenomenon exhibited in Figure 1 as *class bias amplification*. This exacerbated bias arises from local structural disparities between nodes in different classes and is unrelated to other information. Graph structural bias problems have been studied in previous works (Tang et al., 2020; Kang et al., 2022; Liu et al., 2023b; Wang et al., 2022). However, they focused on the structure of individual nodes such as degrees and the distance to class boundaries. Class bias amplification studied in this work should also be distinguished from the class imbalance problem (Song et al., 2022). Although both consider the collective bias of class, works on class-imbalanced classification focus on (semi-)supervised learning and aim to reduce prediction bias caused by imbalanced label distributions. However, class bias amplification occurs in GNN-based GRL and is present even when the label distribution is balanced.

This paper investigates the following two questions: 1. *Why class bias amplification exists in existing GNN-based GRL methods?* 2. *Can we design new unsupervised GRL models to alleviate this issue?* To answer the first question, we analyze the structural bias problem from a spectral perspective, which provides a theoretical explanation on the causes of class bias amplification in existing GNN-based GRL models. There have been numerous works conducting spectral analysis of GNNs, e.g., (Kipf & Welling, 2017; Wu et al., 2019; Oono & Suzuki, 2020; Rong et al., 2020). However, existing analyses mainly focus on the global behaviour: They try to characterize the distribution of node representations using the spectrum of the message passing operator. We point out that this is not suitable when structural bias exists across different regions of the graph. If the number of layers in a GNN is not too large as prevalent in real applications, and we define a community as nodes that belong to the same class, then the embedding distributions of different communities are better characterized by their local spectrum. In particular, if the structures of two communities differ a lot, then the second largest eigenvalues of their normalized adjacency matrices can be quite different, which leads to very different convergence speeds to the stationary subspace. As a result, the embedding distributions of the two communities exhibit different levels of concentration. We then show that such an embedding concentration discrepancy can cause unfairness in downstream tasks through a natural statistical model.

Based on the theoretical analysis, we then focus on how to alleviate the class bias amplification. We propose a simple data augmentation technique, namely random graph coarsening, and provide theoretical justifications on the effectiveness. We finally propose an unsupervised graph contrastive learning model, called Random Graph Coarsening Contrastive Learning (RGCCCL), which utilizes random graph coarsening as data augmentation and uses a contrastive loss that compares the coarsened graph with the original graph. Empirical results on real datasets show our model effectively reduce performance disparities between different classes and also achieves better overall accuracy than baselines, confirming our theoretical analyses.

Our contributions are summarized as follows:

1. We uncover the class bias amplification in the graph and analyze the causes of this problem from a spectral perspective. We show that local structural bias leads to embedding concentration discrepancy, which is harmful on downstream tasks in terms of fairness.
2. We show that an appropriately designed random graph coarsening algorithm can be used as an effective data augmentation tool for alleviating the issue of embedding density imbalance.
3. Based on our theoretical analysis, we propose a novel GCL model RGCCL. Our model mitigates class bias amplification by comparing the coarsened graph with the original graph.
4. We compare RGCCL with other graph representation learning models in various datasets. Empirical experiments and quantitative analysis demonstrate the advantage of RGCCL, which confirms the effectiveness of using random coarsening to mitigate class bias amplification.

2 Preliminaries

Notation. Consider an undirected graph $G = (V, E, X)$, where V represents the vertex set, E denotes the edge set, and $X \in \mathbb{R}^{n \times \mathcal{D}}$ is the feature matrix. Let $n = |V|$ and $m = |E|$ represent the number of vertices and edges, respectively. We use $A \in \{0, 1\}^{n \times n}$ to denote the adjacency matrix of G and $\{v_i, v_j\}$ to denote the undirected edge between node v_i and node v_j . The degree of node v_i denoted as d_i is the number of edges incident on v_i . The degree matrix D is a diagonal matrix and its i -th diagonal entry is d_i .

Graph neural network. In each layer of a GNN, the representation of a node is computed by recursively aggregating and transforming representation vectors of its neighboring nodes from the last layer. One special case is the Graph Convolutional Network (GCN) (Kipf & Welling, 2017). The layer-wise propagation rule of GCN is:

$$H^{(l+1)} = \sigma \left(\tilde{D}^{-\frac{1}{2}} \tilde{A} \tilde{D}^{-\frac{1}{2}} H^{(l)} W^{(l)} \right), \quad (1)$$

where $\tilde{A} = A + I$, $\tilde{D} = D + I$ and $W^{(l)}$ is a learnable parameter matrix. GCNs consist of multiple convolution layers of the above form, with each layer followed by an activation σ such as Relu.

Graph coarsening. The coarse graph is a smaller graph $G' = (A', X')$. G' is obtained from the original graph by computing a partition P of V . The partition can be represented by a binary matrix $P \in \{0, 1\}^{n \times n'}$, with $P_{ij} = 1$ if and only if vertex i belongs to cluster j . We define S as the set of super-node and for each super-node $i \in S$, S_i as the set of nodes that make up the super-node i . I_u is the index of which supernode node u belongs to.

Convergence of Graph Neural Networks There has been lots of work investigating the asymptotic behavior of GNNs as the number of layers L goes to infinity, e.g., (Oono & Suzuki, 2020; Rong et al., 2020). The general conclusion is that as $L \rightarrow \infty$, the representations of all nodes converge to a 1-dimensional subspace, assuming the graph G is connected. The convergence speed is determined by the second largest eigenvalue of the message passing operator \hat{A} . Following the notation from Oono & Suzuki (2020), we denote the maximum singular value of $W^{(l)}$ by ω_l and set $\omega := \max_{l \in [L]} \omega_l$ and assume that $W^{(l)}$ of all layers are initialized so that $\omega \leq 1$. Given a subspace \mathcal{M} , we use $d_{\mathcal{M}} := \inf_{Y \in \mathcal{M}} \|X - Y\|_F$ to measure the closeness between X and \mathcal{M} , where $\|\cdot\|_F$ denote the Frobenius norm. Oono & Suzuki (2020) shows that if G is connected, there is a 1-d subspace \mathcal{M} such that for all l

$$d_{\mathcal{M}}(H^{(l+1)}) \leq \omega \lambda d_{\mathcal{M}}(H^{(l)}), \quad (2)$$

which means the embeddings of all nodes collapse to \mathcal{M} exponentially fast.

3 Exploring Class Bias Amplification

In this section, we analyze the reasons for class bias amplification. We initially explore how local structural biases result in discrepancies in embedding concentration. Then, we demonstrate that such discrepancies can cause unfairness in classification tasks.

3.1 Illustration of Embedding Concentration Discrepancy

In real applications, the number of layers L is typically small. In these cases, the asymptotic results from Eq.(2) do not provide accurate predictions of the model behavior. In particular, they ignore structural differences between different regions of the graph. Here, we illustrate the problem through a simple example. We consider the following example. There are two classes of nodes in the graph, which form the communities C_1 and C_2 , with all nodes within each community belonging to the same class. C_1 is more densely connected than C_2 , and there are only loose connections between them (see the Figure 2). Then, the expression of the symmetric normalized adjacency matrix \hat{A} can be succinctly represented using a block matrix as follows:

$\begin{bmatrix} \hat{A}_1 & \hat{B}_1 \\ \hat{B}_2 & \hat{A}_2 \end{bmatrix}$, where the matrix is partitioned according to C_1 and C_2 . By the assumption, $\|\hat{B}_1\|_F$ and $\|\hat{B}_2\|_F$

are close to 0, and since C_1 has a better connectivity than C_2 , the second largest eigenvalue of \hat{A}_1 , denoted by $\lambda(\hat{A}_1)$ is smaller than $\lambda(\hat{A}_2)$ (Chung & Graham, 1997). According to (2), the representations of all nodes converges to \mathcal{M} with speed exponential in $\lambda(\hat{A})$. A more detailed analysis presented below shows that, the two communities exhibit different convergence speed in the first few layers, due to different local connectivities.

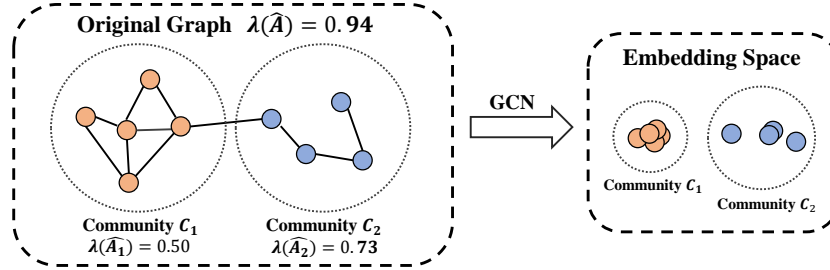


Figure 2: A simple example of embedding density imbalance.

Following the message passing mechanism in Eq.(1), the representations for community C_1 and C_2 can be defined as $H_1^{(l+1)} = \sigma(\hat{A}_1 H_1^{(l)} W^{(l)} + \hat{B}_1 H_2^{(l)} W^{(l)})$ and $H_2^{(l+1)} = \sigma(\hat{A}_2 H_2^{(l)} W^{(l)} + \hat{B}_2 H_1^{(l)} W^{(l)})$, respectively. Since $\|\hat{B}_1\|_F$ and $\|\hat{B}_2\|_F$ are very close to 0, the impact of $H_2^{(l)}$ on $H_1^{(l+1)}$ and $H_1^{(l)}$ on $H_2^{(l+1)}$ is very small. Based on the result of Oono & Suzuki (2020), we have:

$$\begin{cases} d_{\mathcal{M}}(H_1^{(l+1)}) \approx d_{\mathcal{M}}(\sigma(\hat{A}_1 H_1^{(l)} W^{(l)})) \leq \omega \lambda(\hat{A}_1) d_{\mathcal{M}}(H_1^{(l)}), \\ d_{\mathcal{M}}(H_2^{(l+1)}) \approx d_{\mathcal{M}}(\sigma(\hat{A}_2 H_2^{(l)} W^{(l)})) \leq \omega \lambda(\hat{A}_2) d_{\mathcal{M}}(H_2^{(l)}), \end{cases} \quad (3)$$

When the number of iterations L is relatively small as in many real applications, the effects of \hat{B}_1 and \hat{B}_2 can be ignored, and the embedding distributions of different regions $d_{\mathcal{M}}(H_1^{(L)})$ and $d_{\mathcal{M}}(H_2^{(L)})$ are much better characterized by local connectivity (3). Therefore, the embedding density of each community is primarily determined by nodes that constitute the community.

If the structure of communities C_1 and C_2 differs dramatically, for example, $\lambda(\hat{A}_1) \ll \lambda(\hat{A}_2)$, then after L layers of message passing, we have $d_{\mathcal{M}}(H_1^{(L)}) \ll d_{\mathcal{M}}(H_2^{(L)})$. This means the embeddings of nodes in C_1 will be much more concentrated than those in C_2 . In other words, the disparity in local convergence speeds leads to an imbalance in local embedding densities. Figure 2 provides an example of this phenomenon. We sample feature vectors for nodes in C_1 and C_2 from normal distributions, $\mathcal{N}(\begin{bmatrix} -1 \\ -1 \end{bmatrix}, \begin{bmatrix} 1 & 0 \\ 0 & 1 \end{bmatrix})$ and $\mathcal{N}(\begin{bmatrix} 1 \\ 1 \end{bmatrix}, \begin{bmatrix} 1 & 0 \\ 0 & 1 \end{bmatrix})$, respectively. We then apply a 2-layer graph convolutional network, and the resulting embeddings of the nodes are visualized. Even though the node features for C_1 and C_2 are sampled with the same variance, the variance of their embeddings differs due to the convergence bias resulting from the distinct structures.

To further illustrate the differences in the variances of their embeddings, we provide a more quantitative analysis based on the contextual stochastic block model (CSBM) (Deshpande et al., 2018). CSBM is a widely

used statistical model for analyzing expressive power of GNNs (Baranwal et al., 2021; Wu et al., 2022). We consider a two-block CSBM denoted as $\mathcal{G}(n, p_1, p_2, q, \mu_1, \mu_2, \sigma^2)$. Here, $A \in \mathbb{R}^{n \times n}$ represents the adjacency matrix of the graph, and $X \in \mathbb{R}^{n \times d}$ represents the feature matrix. In this model, for any two nodes in the graph, the intra-class probability is denoted as p_i ($i = 1, 2$), and the inter-class probability is denoted as q . Additionally, each node's initial feature is independently sampled from a Gaussian distribution $\mathcal{N}(\mu_i, \sigma^2)$.

Our objective is to estimate the variance of node embeddings within each class. Formally, we aim to compute:

$$\mathbb{E} \left[\|D^{-1}AX - \mathbb{E}(D^{-1}AX)\|_F^2 \right]. \quad (4)$$

Assumption 3.1 (Structural Information). $p_1, p_2, q = \Omega(\frac{\log n}{n})$ and $p_1 > p_2 > q$.

Lemma 3.1. Assume that $d > \frac{C}{\epsilon^2} \log n$, we have $(1 - \epsilon)\|A - \mathbb{E}A\|_F^2 \leq \|AX - \mathbb{E}AX\|_F^2 \leq (1 + \epsilon)\|A - \mathbb{E}A\|_F^2$ with probability at least $1 - 2\exp(-c\epsilon^2 d)$.

Proof. Let $X \in \mathbb{R}^{n \times d}$ be the projection matrix which maps each vector $A_i \in \mathbb{R}^n$ to a d -dimensional vector $A_i X \in \mathbb{R}^d$. Then according to the Johnson-Lindenstrauss lemma (Johnson & Lindenstrauss, 1984), given some tolerance ϵ , it holds with probability at least $1 - 2\exp(-c\epsilon^2 d)$. \square

Lemma 3.2. For a given Erdős-Rényi (ER) graph $\mathcal{G}(n, p)$, there exists a constant C such that $\|A - \mathbb{E}A\| \lesssim C\sqrt{np}$ with probability at least $1 - n^{-r}$ for any $r > 0$.

Proof. By using corollary 3.12 from (Bandeira & van Handel, 2016), we obtain sharper bounds. \square

Lemma 3.3 (Sharp concentration, Lemma 3.2 and Theorem 3 from (Wu et al., 2022)). There exists a constant C such that for sufficiently large n , with probability at least $1 - O(n^{-r})$,

$$\|D^{-1}A - \mathbb{E}(D^{-1}A)\|_F \lesssim \frac{C}{\sqrt{np}}. \quad (5)$$

Theorem 3.4. Given an CSBM $\mathcal{G}(n, p_1, p_2, q, \mu_1, \mu_2, \sigma^2)$, it holds that for the variance of class I with intra-class probability p_1 is smaller than the the variance of class II with intra-class probability p_2 .

Proof. According to Lemma 3.1, to measure the variance of node embedding, we just need to consider structure influence $\|D^{-1}A - \mathbb{E}(D^{-1}A)\|_F^2$. By expressing $A = \begin{bmatrix} A_1 & B \\ B & A_2 \end{bmatrix}$, this allows us to focus on ER graph $\mathcal{G}(\frac{n}{2}, p_i)$ for each class separately. Denote $R_1 = D^{-1}A_1 - \mathbb{E}(D^{-1}A_1)$ and $R_2 = D^{-1}A_2 - \mathbb{E}(D^{-1}A_2)$. We have

$$\|R_1\|_F^2 \leq (1 + \epsilon_1) \frac{C}{np_1} \leq (1 - \epsilon_2) \frac{C}{np_2} \leq \|R_2\|_F^2 \quad (6)$$

for appropriate ϵ_1, ϵ_2 . It follows that variance of node embedding decreases more rapidly for the denser class. Furthermore, the convergence speed is inversely proportional to the intra-probability p_i . \square

3.2 From Embedding Concentration Discrepancy to Class Bias Amplification

We have discussed how different local convergence speeds lead to varying degrees of dispersion in local embedding distributions, and next we provide a theoretical justification on why this can lead to class bias amplification in downstream tasks.

To illustrate the issue, we consider a binary classification problem. Following the setting in Section 3.1, the graph contains two classes of nodes, which form the distinct communities C_1 and C_2 . We assume that the node embeddings from each community follow a Gaussian distribution. We consider the optimal Bayes classifier for the above model, which is known to be the *quadratic discriminant rule*.

Definition 1 (Quadratic Discriminant Analysis). For a binary classification problem, where class 1 has mean μ_1 and variance Σ_1 and class 2 has mean μ_2 and variance Σ_2 . Each sample is drawn from either one with equal probability. Given a new sample x , the QDA rule is

$$\arg \max_{c=1,2} -\frac{1}{2} \log \det \Sigma_c - \frac{1}{2} (x - \mu_c)^T \Sigma_c^{-1} (x - \mu_c). \quad (7)$$

To simplify the discussion, we focus on the one-dimensional case, while the results for higher dimensions are similar. More specifically, each sample x is drawn from $\mathcal{N}(\mu_1, \sigma_1^2)$ or $\mathcal{N}(\mu_2, \sigma_2^2)$ with equal probability, and let y be the label of x . Assume $\sigma_1 \neq \sigma_2$, meaning the data distribution of one class is more concentrated than the other, which models the embedding density imbalance. For this simple case, the optimal classification error can be represented as a closed form.

Proposition 1. *For the above QDA classifier, the error probability of samples from class 1 is:*

$$p_1 = \mathbb{P}(Y^2 > \frac{(\sigma_1^2 + \sigma_2^2)^2}{\sigma_2^2 - \sigma_1^2} - (\sigma_2^2 - \sigma_1^2) + 2\sigma_1^2\sigma_2^2\log(\frac{\sigma_2^2}{\sigma_1^2})), \quad (8)$$

where $Y \sim \mathcal{N}(\sqrt{|\sigma_2^2 - \sigma_1^2|} + (2I(\sigma_1 > \sigma_2) - 1)\frac{\sigma_1^2 + \sigma_2^2}{\sqrt{|\sigma_2^2 - \sigma_1^2|}}, |\sigma_1^2 - \sigma_2^2|\sigma_1^2)$.

The classification error probability of class 2 is symmetric and thus omitted. The above expression is quite complicated. To demonstrate the class bias amplification issue, we define the degree of class bias as $\kappa = \frac{\max\{p_1, p_2\}}{\min\{p_1, p_2\}}$ (larger κ means more severe class bias issue), and investigate how the imbalance in data distribution affects κ . To this end, we fix the value of $\sigma_1^2 + \sigma_2^2$, and vary the ratio σ_1/σ_2 .

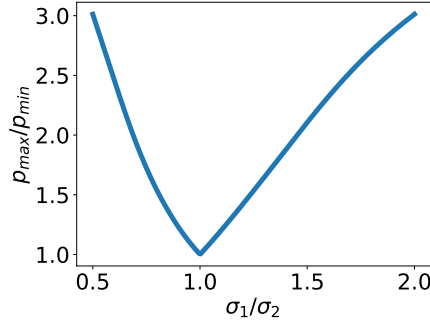


Figure 3: Fairness κ vs. ratio between variances.

The value of κ corresponding to different ratios is plotted in Figure 3. It is evident that as the degree of imbalance in σ_1/σ_2 increases, κ also increases. That is to say, as the degree of imbalance in embedding density grows, the class bias gradually increases as well. Overall, local structural differences exacerbate the embedding concentration discrepancy, which further leads to the amplification of class bias in the classifier.

4 Random Graph Coarsening Contrastive Learning

In this section, we first present the main idea and theoretical justifications of random coarsening to alleviate the class bias amplification. Additionally, we propose the Random Graph Coarsening Contrastive Learning (RGCCL) model, which utilizes random graph coarsening as data augmentation.

4.1 Mitigating Class Bias Amplification via Random Coarsening

Our goal is to make the embedding distribution of sparse classes more concentrated. For this to happen, we first randomly partition the graph into clusters $S = \{S_1, \dots, S_t\}$ according to some random process. Let f be a GNN encoder, and $f(u)$ be the embedding of node u . We define the embedding for a cluster S_i as $f(S_i) = \frac{1}{|S_i|} \sum_{v \in S_i} f(v)$. We use the loss

$$\sum_{S_i \in S} \sum_{u \in S_i} \|f(u) - f(S_i)\|^2 \quad (9)$$

to regularize the GNN encoder, which encourages nodes in each cluster in the random partition to be more concentrated. In the following, we first show that if the distribution of the random partition, denoted

by \mathcal{P} , satisfies certain requirements, the above loss has the implicit effect of pushing the embeddings of sparse classes more heavily. Then, we provide a specific random partition algorithm, namely random graph coarsening, which meets the requirements.

Following the setting in Section 3.2, we consider a binary classification problem. Assume that for a random partition drawn from \mathcal{P} , the probability that two nodes from class 1 (class 2) lie in the same cluster is q_1 (q_2), and the probability that two nodes from different classes are clustered together is q_{12} . We have the following lemma, the proof of which is provided in the appendix A.1.

Lemma 4.1. *Let C_1 and C_2 be the two classes of nodes. Suppose each cluster has the same size s , then*

$$\begin{aligned} & \mathbb{E}_{P \sim \mathcal{P}} \sum_{S_i \in S} \sum_{u \in S_i} s \|f(u) - f(S_i)\|^2 \\ &= q_1 \sum_{u, v \in C_1, u \neq v} \|f(u) - f(v)\|^2 + q_2 \sum_{u, v \in C_2, u \neq v} \|f(u) - f(v)\|^2 \\ &+ q_{12} \sum_{u \in C_1, v \in C_2} \|f(u) - f(v)\|^2. \end{aligned}$$

Now suppose C_1 is denser than C_2 , and by the analysis in Section 3.1, the embeddings in C_1 are likely to be more concentrated. To make the embedding densities of C_1 and C_2 more balanced, from Lemma 4.1, a preferred random partitioning algorithm should satisfy

$$q_2 > q_1 > q_{12}. \quad (10)$$

Here, we design a random graph coarsening strategy to obtain such a reasonable partition, which can satisfy (10). Due to the homophily principle that similar nodes may be more likely to attach to each other than dissimilar ones, if we always merge nodes that are connected by an edge, q_{12} should be less than q_1 and q_2 . On average, the degrees of nodes in C_2 are lower than C_1 . To realize $q_2 > q_1$, we adopted a simple probability function $\omega(u, v) = \frac{1}{d_u + d_v}$ for random edge selection during coarsening, ensuring a higher probability for low-degree nodes to participate in the random coarsening. Specifically, we first compute $\omega(u, v)$ to construct the weight set \mathcal{I} of all edges, and then determine the edges to be coarsened by randomly selecting edges according to the weight set \mathcal{I} .

Therefore, our random graph coarsening strategy iteratively merging two (super) nodes through edge contraction to form more super nodes. Eventually, we can obtain a coarsened graph, where each supernode represents a cluster, and the nodes that constitute this supernode belong to the same partition. By contrasting the nodes in the original graph with their corresponding supernodes (clusters) in the coarsened graph, we can optimize loss (9) to mitigate class bias amplification. To prevent the formation of large supernodes, we use a threshold limiting the size of supernodes during the coarsening process. A detailed description of our random coarsening algorithm is provided in the appendix A.4.

4.2 Framework of RGCCL

Based on the theoretical insights from Section 4.1, we present a novel multi-view graph contrastive learning method RGCCL, which can effectively alleviate the issue of class bias amplification. Compared to existing GCL models, the key difference in our approach is to use random graph coarsening as the graph augmentation method and a specially designed loss function for this framework.

The GCL method generates different views through graph augmentation, and then trains the model parameters by comparing the node embeddings from different views. The architecture of RGCCL is presented in Figure 4. In our RGCCL, we regard the original graph as one view and the coarsened graph as another view, and then compare the corresponding nodes in these two views. In order to alleviate class bias amplification, we need to push the node embedding $f(u)$ towards its corresponding cluster center embedding $f(S_u)$ according to the analysis in Section 4.1. Specifically, the super-node embedding computed in the coarsened view is used as the cluster center, and then each node embedding in the original graph and its corresponding

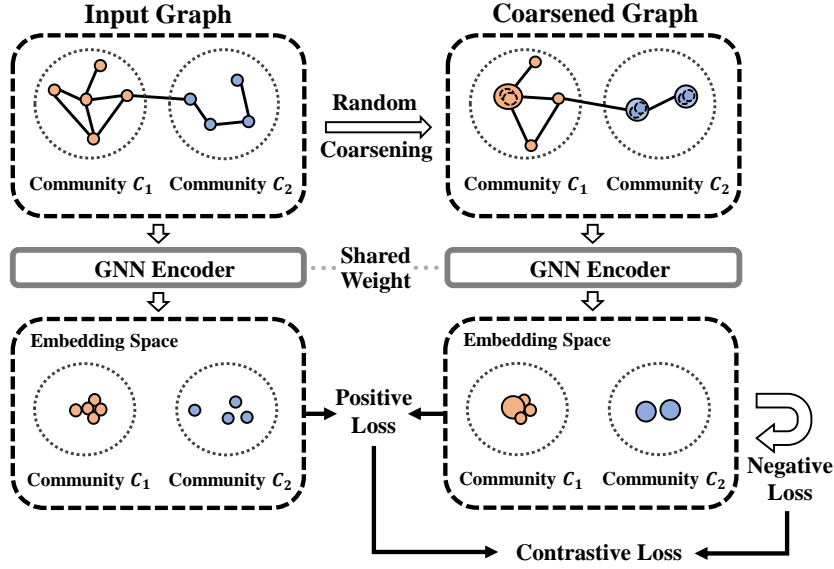


Figure 4: The architecture of the proposed RGCCL.

super-node embedding in the coarsened graph is defined as a positive pair. By conducting contrastive learning on such positive pairs, we make the embedding distribution of sparse classes more concentrated, thereby reducing class bias amplification.

In this work, we use a method different from the previous graph coarsening algorithms (Huang et al., 2021) to construct the coarsened feature matrix. A difference is that they construct the new feature matrix simply by summing i.e., given a partition matrix P , $X' = P^T X$. Here, a normalization based on degrees is applied: $X' = \tilde{D}'^{-1} P^T \tilde{D} X$, where \tilde{D}' and \tilde{D} are the degree matrices of the two views. The purpose is to ensure, as the number of graph propagations goes to infinity, the embedding of a node and its corresponding supernode in the coarsened view converge to the same point. This computational method is supported by the following upper bound

$$\|Z_u - Z'_v\| \leq \kappa \sqrt{\frac{d_{max}}{d_{min}}} (n\lambda_2^k + n'\lambda_2'^k). \quad (11)$$

Here, u represents a node in the original graph, while v is its corresponding node in the coarsened graph. We denote the node embeddings learned from the original graph G and the coarsened graph G' as Z_u and Z'_v , respectively. λ_2 and λ_2' are the second largest eigenvalues in G and G' respectively. d_{max} and d_{min} are the maximum degree and minimum degree in G and G' , respectively. A detailed proof can be found in Appendix A.2.

On the other hand, graph coarsening is a method of data reduction, so using random graph coarsening as data augmentation can also reduce the resource consumption of GNN training, especially when computing positive and negative sample pairs.

Specifically, we apply the random graph coarsening algorithm to generate one graph augmentation $G' = (A', X')$ in each epoch during training. Then, we compute the coarsened graph and original graph embeddings by a GNN encoder with shared parameters: $H = \text{GNN}(A', X', \theta)$ and $Z = \text{GNN}(A, X, \theta)$.

Recall that positive pairs are of the form (u, S_u) , where S_u denotes the corresponding supernode of u . So we penalize $\|Z_u - H_{S_u}\|_F^2$. The loss function of positive pairs can be described more concisely in the matrix form. Let $Z' = PH$, then $Z'_u = H_{S_u}$. Therefore, the positive pair loss function is

$$\mathcal{L}_{pos} = \|Z - Z'\|_F^2 = \|Z\|_F^2 + \|Z'\|_F^2 - 2\text{Tr}(Z^T Z'). \quad (12)$$

If Z and Z' are normalized appropriately, we only need to minimize $-2\text{Tr}(Z^T Z')$.

Considering that the node embeddings Z derived from the original graph G may encounter imbalance issues, whereas the coarsened graph G' typically exhibits a more balanced embedding distribution. Therefore, we do not pick negative pairs from the original graph and only compute a negative pair loss with the coarsened graph. There are various methods for selecting negative pairs and computing the loss; here we use the loss from Zhang et al. (2020), which is derived from the graph partition problem. More specifically, we randomly sample a small set of supernode pairs $\mathcal{N}' \subset V' \times V'$, and the negative pair loss function is:

$$\mathcal{L}_{neg} = \frac{\alpha}{\sum_{(i,j) \in \mathcal{N}'} n_i n_j \|h_i - h_j\|^2}. \quad (13)$$

where h_i and h_j are the embeddings of supernodes i and j , and n_i and n_j are the number of original nodes contained in supernodes i and j .

Optimizing $\mathcal{L}_{neg} + \mathcal{L}_{pos}$ will be difficult due to the huge difference of the scale of \mathcal{L}_{pos} and \mathcal{L}_{neg} . Therefore, we transform \mathcal{L}_{pos} into the following form

$$\mathcal{L}_{pos} = \frac{\beta}{\text{Tr}(Z^T Z')}. \quad (14)$$

Finally, the loss function of our model is

$$\mathcal{L} = \frac{\alpha}{\sum_{(i,j) \in \mathcal{N}'} n_i n_j \|h_i - h_j\|^2} + \frac{\beta}{\text{Tr}(Z^T Z')}. \quad (15)$$

4.3 Generalizability of RGCCL

The generalizability of self-supervised learning methods has recently been theoretically analyzed in (Huang et al., 2023; Wang et al., 2022). They characterize it with three properties, namely the concentration of augmented data, the alignment of positive samples and the divergence of class centers. Huang et al. (2023) also shows that the divergence of class centers is controlled by classic contrastive losses such as InfoNCE and the cross-correlation loss.

Following the proof of Huang et al. (2023), we show that our self-supervised loss \mathcal{L}_{neg} can also upper bounds the divergence of class centers, thus classes will be more separable if our objective is optimized. The theorem is stated as follows, with further details provided in Appendix A.3.

Theorem 4.2. *Assume that encoder f with norm 1 is M -Lipschitz continuous. For a given $(\alpha, \gamma, \hat{d})$ augmentation set A , any $\epsilon > 0$ and $k \neq l$,*

$$\mu_k^T \mu_l \leq \frac{1}{p_k p_l} \left(-\frac{1}{2n^2 \mathcal{L}_{neg}} + \tau(\epsilon, \alpha, \gamma, \hat{d}) \right), \quad (16)$$

where $\tau(\epsilon, \alpha, \gamma, \hat{d}) = 2R_\epsilon + 16(1 - \alpha(1 - \frac{1}{2}\epsilon - \frac{1}{4}M \max_k(\gamma \sqrt{\frac{\mathcal{D}}{d_{\min}^k}})) + KR_\epsilon)^2 + 8(1 - \alpha(1 - \frac{1}{2}\epsilon - \frac{1}{4}M \max_k(\gamma \sqrt{\frac{\mathcal{D}}{d_{\min}^k}})) + KR_\epsilon + \frac{K-1}{K})$.

Next we discuss the concentration property of the random coarsening augmentation. First notice that for any two nodes u and v , the probability that they are coarsened together is equal to the probability that they are connected by randomly selected edges in the algorithm. Suppose the edges are selected independent and identically with probability p , then the connection probability is lower bounded by $p^{\text{dia}(G)}$, where $\text{dia}(G)$ is the diameter of G . Once u and v are coarsened together in at least one coarsened graph, $d(u, v) = 0$, which means our random coarsening augmentation can be very well-concentrated.

5 Related Work

Contrastive learning on graphs. Contrastive learning is a type of unsupervised learning technique that learns a representation of data by differentiating similar and dissimilar samples. It has been used

in a variety of applications within the domain of graph data. DGI (Velićković et al., 2018) and MVGRL (Hassani & Ahmadi, 2020) contrast node embeddings with graph embeddings using a loss function based on mutual information estimation (Belghazi et al., 2018; Hjelm et al., 2019). GRACE (Zhu et al., 2020) and its variants (Zhu et al., 2021; You et al., 2020) aim to maximize the similarity of positive pairs and minimize the similarity of negative pairs in augmented graphs in order to learn node embeddings. To counter the performance degradation induced by false negative pairs, CCA-SSG (Zhang et al., 2021) simplifies the loss function by eliminating negative pairs. In order to reduce the computational complexity of contrastive loss, GGD (Zheng et al., 2022) discriminates between two groups of node samples using binary cross-entropy loss. For a broader understanding, we recommend that readers refer to the latest surveys (Liu et al., 2023a; Xie et al., 2023).

Structural bias on graphs. Fair graph mining has attracted much more research attention since recent studies reveal that there are unfairness in a large number of graph mining models. Several notions of fairness have been proposed in recent survey (Dong et al., 2023), and structural bias is mainly manifested as degree bias. Prior studies (Tang et al., 2020; Kang et al., 2022; Dong et al., 2022; Liu et al., 2023b) have primarily concentrated on degree bias in supervised graph learning. GRADE (Wang et al., 2022) first focuses on structural bias in unsupervised graph representation learning, mitigating the degree bias issue through a degree-based graph data augmentation method. In view of the wide application of GNN-based graph representation learning, the structural bias problem associated with it should receive more attention from researchers. Existing studies on bias amplification, such as those in computer vision and NLP (Zhao et al., 2017; Wang & Russakovsky, 2021; Hall et al., 2022), have not considered graph structural bias, and their definitions of bias amplification are primarily based on output distribution shifts rather than structural propagation. Different from them, we are the first to study the phenomenon of class bias amplification on graphs, which specifically captures how initial class imbalances are progressively exacerbated by GNN structures, rather than demographic or attribute biases commonly discussed in prior works.

Graph coarsening. Recently, graph coarsening techniques have been used to address issues in graph neural networks (Fahrbach et al., 2020; Deng et al., 2019; Huang et al., 2021; Jin et al., 2022; Yang et al., 2025). Graph coarsening with spectral approximation guarantees are studied in (Li & Schild, 2018; Loukas, 2019; Jin et al., 2020). Graph coarsening can reduce the size of graph by combining the similar nodes, then the coarsened graph can be used for downstream tasks related to the graph. Existing graph coarsening techniques primarily strive to maintain the overall graph structure, resulting in a static and downsized coarsened graph. These methods overlooks the local structural bias, and typically involves massive computational costs.

6 Experiments

6.1 Experimental Setup

Datasets. The results are evaluated on six real-world datasets (Kipf & Welling, 2017; Velićković et al., 2018; Zhu et al., 2021; Hu et al., 2020), Cora, Citeseer, Pubmed, Amazon Computer, Amazon Photo, and Ogbn-Arxiv. Graph representation learning shows different degrees of class bias in these datasets. More detailed statistics of the six datasets are summarized in Table 7. On small-scale datasets Cora, Citeseer, Pubmed, Photo and Computers, performance is evaluated on random splits. We select 20 labeled nodes per class for training, while the remaining nodes are used for testing. For Ogbn-Arxiv, we use fixed data splits as in previous studies Hu et al. (2020).

Baselines. We compare our approach against ten representative graph embedding models: Deepwalk (Perozzi et al., 2014), DGI (Velićković et al., 2018), GraphCL (You et al., 2020), GRACE (Zhu et al., 2020), GCA (Zhu et al., 2021), CCA-SSG (Zhang et al., 2021), gCool (Li et al., 2022), GRADE (Wang et al., 2022), GGD (Zheng et al., 2022), SPAN (Lin et al., 2023) and PolyGCL (Chen et al., 2024). For all the baselines, we use the public code released in their previous papers. All models evaluate the learned representations by training and testing classifiers with the same settings. More experimental details are listed in the appendix A.5.

6.2 Results and Analysis

Table 1 reports the node classification performance on small datasets. In these data splits, we employ Acc and Macro-F1 as metrics to assess the overall performance of models. If Macro-F1 significantly drops compared to Acc, it indicates that the model’s performance is not balanced across different classes. It is evident that the performance of RGCCL outperforms other GRL models within the given experimental framework. Mostly, RGCCL surpasses the runner-up by an advantage of 1%-2%. Notably, although RGCCL’s Acc score on the Computers dataset is slightly lower than that of CCA-SSG, our Macro-F1 score is significantly higher than that of CCA-SSG. This suggests that CCA-SSG has generated significant class bias on Computers. Clearly, our specially designed model can improve the overall classification performance effectively while resolving the issue of class bias amplification.

Table 1: Summary of results in terms of mean node classification accuracy and standard deviation over 50 runs on five datasets.

Method	Cora		Citeseer		Pubmed		Photo		Computers	
	Acc	Macro-F1	Acc	Macro-F1	Acc	Macro-F1	Acc	Macro-F1	Acc	Macro-F1
Deepwalk	67.2±1.7	66.5±1.5	40.0±2.1	38.3±2.0	66.9±2.8	65.6±2.7	85.1±1.2	83.9±1.2	77.3±1.6	77.2±1.5
DGI	78.5±0.9	77.2±0.9	70.4±1.0	63.6±1.4	72.5±3.3	72.5±3.3	87.9±1.3	86.2±1.3	79.7±1.6	78.4±1.3
GraphCL	78.3±1.5	76.7±1.7	70.6±1.2	64.1±1.4	71.7±3.5	71.7±3.6	88.3±1.3	86.7±1.2	79.7±1.4	78.5±1.1
GRACE	74.4±2.0	72.5±2.0	68.9±1.0	61.2±1.1	76.1±2.8	75.9±2.7	85.1±1.6	83.5±1.4	76.2±1.9	75.2±1.5
GCA	78.6±1.2	77.2±1.2	68.8±1.5	65.3±1.4	75.4±3.0	75.5±2.9	87.8±1.2	86.2±1.3	79.1±2.4	77.9±2.0
CCA-SSG	79.2±1.4	78.0±1.4	71.8±1.0	66.3±1.1	76.0±2.8	75.8±2.7	88.7±1.1	86.9±3.2	82.7±1.0	76.9±3.7
gCooL	78.5±1.3	77.1±1.1	68.6±1.4	64.9±1.3	75.5±3.0	75.3±2.9	87.9±1.3	85.9±1.4	79.8±1.7	78.1±1.3
GRADE	81.5±1.0	80.2±1.0	67.6±1.5	64.2±1.3	74.5±2.7	74.5±2.6	87.1±1.2	80.4±3.0	75.8±1.2	64.7±3.1
GGD	81.9±0.9	80.5±0.8	70.1±1.3	66.2±1.1	74.7±3.2	74.4±3.1	87.2±1.5	85.4±1.4	80.4±1.8	80.0±1.2
SPAN	80.7±0.6	78.8±0.7	69.1±1.2	64.3±1.1	73.1±2.8	72.6±2.8	86.3±1.5	84.4±1.6	76.4±1.7	75.8±1.4
PolyGCL	77.4±3.2	75.8±3.1	69.9±1.4	62.7±1.3	75.2±3.4	75.5±3.1	85.7±1.4	84.6±1.3	76.7±1.6	75.5±1.5
RGCCL	83.1±0.8	82.0±0.8	72.4±0.9	67.7±0.8	77.3±2.9	77.1±2.7	89.6±1.2	88.2±1.2	81.2±1.8	80.2±1.2

Quantitative analysis. To further demonstrate that RGCCL effectively alleviates the amplification of class bias, we present statistics of the learned representations and compare them with other popular GRL methods. Firstly, we measure the concentration of the embedding for each class by calculating their mean distances from the centroid (i.e., $V_C = \frac{1}{|C|} \sum_{i \in C} \|z_i - \frac{1}{|C|} \sum_{i \in C} z_i\|$ for class C). Next, we compute the average and standard deviation of V_C across all classes. A smaller average value indicates that the representations for each class are more concentrated, which in turn makes the classification boundary easier to learn. A smaller standard deviation suggests a more balanced embedding density, which has been shown to be beneficial for classification fairness (as discussed in Section 3.2). In Table 2, we present the results of four baseline methods as well as RGCCL on Cora and Citeseer. RGCCL demonstrates not only more concentrated embeddings for each class but also the most balanced embedding density. These results strongly support our theory. Furthermore, we use the Matthew’s coefficient to measure class bias. Table 3 presents the results of Matthew’s coefficient for representative GRL models and our RGCCL. The results indicate that the bias in the embeddings learned by RGCCL is significantly less than that of other GRL models.

Visualization. To further illustrate that RGCCL effectively mitigates the issue of class bias amplification, we have visualized the performance of each model across different classes. For each class, we compute the

Table 2: The average and standard deviation of class density. A smaller average indicates higher embedding quality, while a smaller standard deviation suggests less class bias.

Method	Cora		Citeseer	
	Ave	Std	Ave	Std
DGI	0.3782	0.0294	0.3402	0.0255
GRACE	0.2114	0.0252	0.1715	0.0163
CCA-SSG	0.2817	0.1031	0.1672	0.0109
GRADE	0.1983	0.0352	0.2141	0.0243
GGD	0.3183	0.0541	0.3297	0.0329
SPAN	0.3260	0.0323	0.3234	0.0227
RGCCL	0.0942	0.0084	0.1401	0.0097

Table 3: Matthew’s coefficient for RGCCL and six baselines.

	Cora	CiteSeer	PubMed
DGI	73.0 \pm 1.5	64.5 \pm 1.2	57.8 \pm 4.3
GRACE	67.9 \pm 1.6	60.0 \pm 2.0	62.3 \pm 3.8
CCA-SSG	74.5 \pm 1.6	64.6 \pm 1.4	64.0 \pm 4.1
GRADE	75.7 \pm 1.5	62.1 \pm 1.3	58.1 \pm 3.4
GGD	77.0 \pm 1.6	64.9 \pm 1.2	63.7 \pm 4.1
SPAN	76.9 \pm 0.7	62.4 \pm 1.4	60.3 \pm 4.0
RGCCL	78.9\pm0.9	66.3\pm0.8	65.6\pm4.2

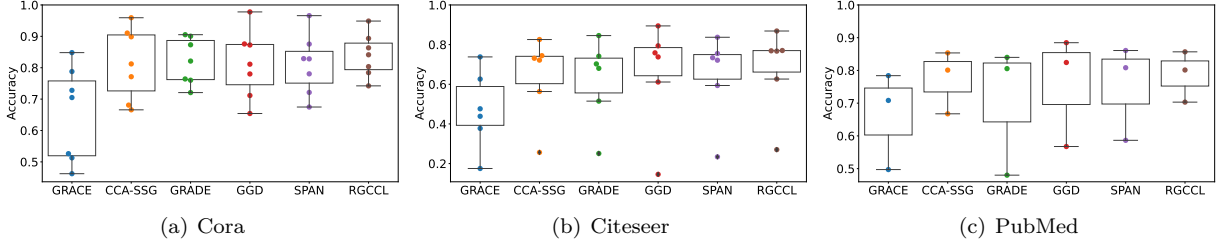


Figure 5: Box plots of the average accuracy w.r.t. class for five baselines and RGCCL on the Cora, Citeseer and Pubmed dataset.

average performance of the model in this class and then draw a box plot based on these accuracies. Figure 5 provides a visualization of the node classification accuracy in different classes on the Cora, Citeseer and PubMed. It is clear that our model has the smallest performance difference across different classes, while also having the best overall performance.

Scalability. Another benefit of RGCCL is its small memory usage. This efficiency is primarily because the random graph coarsening is preprocessed on the CPU, resulting in a coarsened graph notably smaller than the original. Experiments were also conducted on the Arxiv dataset, which is a large-scale dataset for most GRL models. Larger size makes sub-sampling necessary for training on some baselines, but our RGCCL can be trained directly on the full graph. As shown in Table 4, the Acc and Macro-F1 of RGCCL both exceed those of other baselines.

Figure 6 shows the memory usage of our model and seven mainstream GCL models on Citeseer and Pubmed. RGCCL exhibits the same level of memory usage as GGD, which is specifically designed to save computation costs; our model benefits from the effective reduction of graph size via random coarsening.

Effectiveness of different coarsening ratios. We studied the effect of random coarsening ratio on model performance. The random coarsening ratio refers to the proportion of the number of nodes reduced relative to the total number of nodes. Table 5 shows the results of different coarsening ratios. According to our

Table 4: Summary of results in terms of accuracy on Ogbn-Arxiv.

Method	Ogbn-Arxiv	
	Acc	Macro-F1
DGI	68.8 \pm 0.2	46.8 \pm 0.4
GRACE	68.4 \pm 0.1	46.1 \pm 0.3
CCA-SSG	69.8 \pm 0.2	46.5 \pm 0.6
GRADE	67.7 \pm 0.2	45.0 \pm 0.4
GGD	70.7 \pm 0.3	48.5 \pm 0.4
SPAN	70.1 \pm 0.3	48.7 \pm 0.5
RGCCL	71.7\pm0.1	50.6\pm0.2

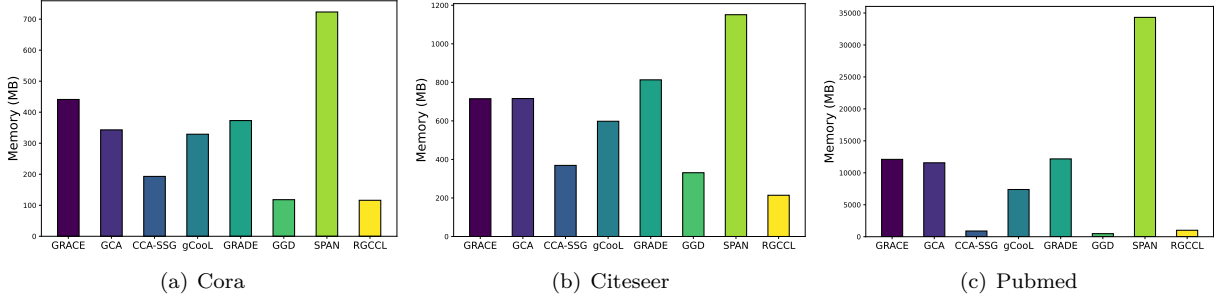


Figure 6: The memory usage of baselines and RGCCL on Cora, Citeseer and Pubmed.

observations, the changes in the coarsening rate have a more significant impact on the Macro-F1. The model performs better when the coarsening rate is between 30% and 50%. If the coarsened graph is too small, it may lead to the loss of information in the augmented graph, which could in turn cause a decline in the performance of the RGCCL.

Table 5: The performance of different coarsening ratio.

Ratio	Cora		Citeseer		Pubmed	
	Acc	Macro-F1	Acc	Macro-F1	Acc	Macro-F1
$r = 0.3$	83.1 \pm 0.8	82.0 \pm 0.8	72.4 \pm 0.9	67.6 \pm 0.8	77.1 \pm 2.9	76.9 \pm 2.7
$r = 0.5$	82.8 \pm 0.8	81.8 \pm 0.8	72.4 \pm 0.9	67.7 \pm 0.8	77.3 \pm 2.9	77.1 \pm 2.7
$r = 0.7$	82.5 \pm 0.9	81.4 \pm 0.9	72.1 \pm 0.7	67.0 \pm 0.7	77.1 \pm 2.8	76.8 \pm 2.6
$r = 0.9$	82.4 \pm 0.9	81.1 \pm 1.0	72.0 \pm 0.7	66.9 \pm 0.7	77.0 \pm 2.8	76.9 \pm 2.6

Table 6: The performance of different loss terms ratio.

Method	Cora		Citeseer		Pubmed	
	Acc	Macro-F1	Acc	Macro-F1	Acc	Macro-F1
RGCCL	83.1 \pm 0.8	82.0 \pm 0.8	72.4 \pm 0.9	67.7 \pm 0.8	77.3 \pm 2.9	77.1 \pm 2.7
RGCCL w/o \mathcal{L}_{neg}	80.8 \pm 0.9	79.8 \pm 0.8	58.0 \pm 3.4	54.6 \pm 2.9	67.7 \pm 6.0	66.9 \pm 6.8
RGCCL w/o \mathcal{L}_{pos}	82.8 \pm 0.8	81.7 \pm 0.7	72.0 \pm 0.8	67.4 \pm 0.7	76.6 \pm 2.8	76.4 \pm 2.6

Effectiveness of different loss terms. We conducted an ablation study to evaluate the contribution of different loss terms in our model. Specifically, we examined the impact of removing the positive loss term \mathcal{L}_{pos} and the negative loss term \mathcal{L}_{neg} on node classification performance. As shown in Table 6, the removal of \mathcal{L}_{neg} leads to a significant drop in performance across all three datasets, especially on Citeseer, where the accuracy and Macro-F1 decrease by about 14% and 13%, respectively. This indicates that \mathcal{L}_{neg} plays a crucial role in preserving discriminative information during training. On the other hand, removing \mathcal{L}_{pos} only causes a slight performance degradation, suggesting that while beneficial, its contribution is less critical compared to \mathcal{L}_{neg} . Overall, the full model achieves the best results, demonstrating the complementary effects of both loss terms.

7 Limitations and Future Work

It is important to emphasize that this study is conducted under the homophilic graph setting, which aligns closely with the mainstream research direction in the field of graph representation learning. This setting ensures that our theoretical framework and methods are well-suited to the widely adopted paradigm—namely, that connected nodes are more likely to share similar attributes. While our method demonstrates excellent performance and robustness under the homophilic assumption, its applicability to heterophilic graphs remains an open question. Heterophilic graphs are characterized by connections between dissimilar nodes, presenting unique challenges that are beyond the scope of this study. In future work, we plan to extend the exploration

of class bias amplification to heterophilic graph settings. This direction will likely require the development of new theoretical tools and the establishment of evaluation metrics tailored to the characteristics of heterophilic graphs.

8 Conclusion

In this paper, we study the issue of class bias amplification in GNN-based graph representation learning. We present a novel perspective on this problem through the lens of convergence bias and embedding concentration discrepancy, and a comprehensive theoretical analysis is provided. Based on our theoretical insights, we propose to use random graph coarsening to mitigate this issue, and give theoretical guidance on how to design effective random coarsening algorithms. Finally, a graph contrastive learning model is proposed which utilize random graph coarsening as graph augmentation and a loss function is designed for this new form of graph augmentation. Comprehensive experimental evaluation illustrates the superiority of RGCCL in mitigating class bias amplification.

Acknowledgments

This work is supported by National Natural Science Foundation of China No. U2241212, No. 62276066, and the Postdoctoral Fellowship Program of CPSF under Grant No. GZC20252742. The computations in this research were performed using the CFFF platform of Fudan University.

References

- Afonso S. Bandeira and Ramon van Handel. Sharp nonasymptotic bounds on the norm of random matrices with independent entries. *The Annals of Probability*, 44(4):2479 – 2506, 2016.
- Aseem Baranwal, Kimon Fountoulakis, and Aukosh Jagannath. Graph convolution for semi-supervised classification: Improved linear separability and out-of-distribution generalization. In *Proceedings of the 38th International Conference on Machine Learning*, pp. 684–693, 2021.
- Mohamed Ishmael Belghazi, Aristide Baratin, Sai Rajeshwar, Sherjil Ozair, Yoshua Bengio, Aaron Courville, and Devon Hjelm. Mutual information neural estimation. In *International Conference on Machine Learning*, pp. 531–540, 2018.
- Aleksandar Bojchevski and Stephan Günnemann. Deep gaussian embedding of graphs: Unsupervised inductive learning via ranking. In *International Conference on Learning Representations*, 2018.
- Jianfei Chen, Jun Zhu, and Le Song. Stochastic training of graph convolutional networks with variance reduction. In *International Conference on Machine Learning*, pp. 942–950, 2018.
- Jingyu Chen, Runlin Lei, and Zhewei Wei. Polygcl: Graph contrastive learning via learnable spectral polynomial filters. In *International Conference on Learning Representations*, 2024.
- Fan RK Chung and Fan Chung Graham. *Spectral graph theory*. American Mathematical Soc., 1997.
- Weilin Cong, Rana Forsati, Mahmut Kandemir, and Mehrdad Mahdavi. Minimal variance sampling with provable guarantees for fast training of graph neural networks. In *ACM SIGKDD international conference on Knowledge Discovery and Data Mining*, pp. 1393–1403, 2020.
- Weilin Cong, Morteza Ramezani, and Mehrdad Mahdavi. On the importance of sampling in learning graph convolutional networks. *arXiv preprint arXiv:2103.02696*, 2021.
- Chenhui Deng, Zhiqiang Zhao, Yongyu Wang, Zhiru Zhang, and Zhuo Feng. Graphzoom: A multi-level spectral approach for accurate and scalable graph embedding. In *International Conference on Learning Representations*, 2019.

- Yash Deshpande, Subhabrata Sen, Andrea Montanari, and Elchanan Mossel. Contextual stochastic block models. In *Advances in Neural Information Processing Systems*, volume 31, pp. 8590–8602, 2018.
- Yushun Dong, Ninghao Liu, Brian Jalaian, and Jundong Li. EDITS: modeling and mitigating data bias for graph neural networks. In *The Web Conference*, 2022.
- Yushun Dong, Jing Ma, Chen Chen, and Jundong Li. Fairness in graph mining: A survey. *TKDE*, 2023.
- Matthew Fahrbach, Gramoz Goranci, Richard Peng, Sushant Sachdeva, and Chi Wang. Faster graph embeddings via coarsening. In *International Conference on Machine Learning*, 2020.
- Vikas Garg, Stefanie Jegelka, and Tommi Jaakkola. Generalization and representational limits of graph neural networks. In *International Conference on Machine Learning*, pp. 3419–3430, 2020.
- Aditya Grover and Jure Leskovec. node2vec: Scalable feature learning for networks. In *Proceedings of the International Conference on Knowledge Discovery and Data Mining*, pp. 855–864, 2016.
- Melissa Hall, Laurens van der Maaten, Laura Gustafson, and Aaron Adcock. A systematic study of bias amplification. *Arxiv*, abs/2201.11706, 2022.
- Kaveh Hassani and Amir Hosein Khas Ahmadi. Contrastive multi-view representation learning on graphs. In *International Conference on Machine Learning*, pp. 4116–4126, 2020.
- R Devon Hjelm, Alex Fedorov, Samuel Lavoie-Marchildon, Karan Grewal, Phil Bachman, Adam Trischler, and Yoshua Bengio. Learning deep representations by mutual information estimation and maximization. In *International Conference on Learning Representations*, 2019.
- Weihua Hu, Matthias Fey, Marinka Zitnik, Yuxiao Dong, Hongyu Ren, Bowen Liu, Michele Catasta, and Jure Leskovec. Open graph benchmark: Datasets for machine learning on graphs. *Advances in neural information processing systems*, pp. 22118–22133, 2020.
- Weiran Huang, Mingyang Yi, and Xuyang Zhao. Towards the generalization of contrastive self-supervised learning. In *International Conference on Learning Representations*, 2023.
- Zengfeng Huang, Shengzhong Zhang, Chong Xi, Tang Liu, and Min Zhou. Scaling up graph neural networks via graph coarsening. In *ACM SIGKDD international conference on Knowledge Discovery and Data Mining*, pp. 675–684, 2021.
- Wei Jin, Lingxiao Zhao, Shichang Zhang, Yozen Liu, Jiliang Tang, and Neil Shah. Graph condensation for graph neural networks. In *International Conference on Learning Representations*, 2022.
- Yu Jin, Andreas Loukas, and Joseph JaJa. Graph coarsening with preserved spectral properties. In *International Conference on Artificial Intelligence and Statistics*, 2020.
- William B. Johnson and Joram Lindenstrauss. Extensions of Lipschitz mappings into a Hilbert space. In *Conference on modern analysis and probability*, volume 26, pp. 189–206, 1984.
- Jian Kang, Yan Zhu, Yinglong Xia, Jiebo Luo, and Hanghang Tong. Rawlsgcn: Towards rawlsian difference principle on graph convolutional network. In *The Web Conference*, 2022.
- Thomas N Kipf and Max Welling. Semi-supervised classification with graph convolutional networks. In *International Conference on Learning Representations*, 2017.
- Bolian Li, Baoyu Jing, and Hanghang Tong. Graph communal contrastive learning. In *The Web Conference*, 2022.
- Huan Li and Aaron Schild. Spectral subspace sparsification. In *IEEE Annual Symposium on Foundations of Computer Science*, 2018.
- Lu Lin, Jinghui Chen, and Hongning Wang. Spectral augmentation for self-supervised learning on graphs. In *International Conference on Learning Representations*, 2023.

- Yixin Liu, Ming Jin, Shirui Pan, Chuan Zhou, Yu Zheng, Feng Xia, and Philip S. Yu. Graph self-supervised learning: A survey. *IEEE TKDE*, 35(6):5879–5900, 2023a.
- Zemin Liu, Trung-Kien Nguyen, and Yuan Fang. On generalized degree fairness in graph neural networks. In *Association for the Advancement of Artificial Intelligence*, 2023b.
- Andreas Loukas. Graph reduction with spectral and cut guarantees. *Journal of Machine Learning Research*, 20(116):1–42, 2019.
- Kenta Oono and Taiji Suzuki. Graph neural networks exponentially lose expressive power for node classification. In *International Conference on Learning Representations*, 2020.
- Bryan Perozzi, Rami Al-Rfou, and Steven Skiena. Deepwalk: Online learning of social representations. In *ACM SIGKDD international conference on Knowledge Discovery and Data Mining*, 2014.
- Yu Rong, Wenbing Huang, Tingyang Xu, and Junzhou Huang. Dropedge: Towards deep graph convolutional networks on node classification. In *International Conference on Learning Representations*, 2020.
- Jaeyun Song, Joonhyung Park, and Eunho Yang. Tam: topology-aware margin loss for class-imbalanced node classification. In *International Conference on Machine Learning*, pp. 20369–20383. PMLR, 2022.
- Xianfeng Tang, Huaxiu Yao, Yiwei Sun, Yiqi Wang, Jiliang Tang, Charu C. Aggarwal, Prasenjit Mitra, and Suhan Wang. Investigating and mitigating degree-related biases in graph convolutional networks. In *International Conference on Information and Knowledge Management*, 2020.
- Petar Veličković, William Fedus, William L Hamilton, Pietro Liò, Yoshua Bengio, and R Devon Hjelm. Deep graph infomax. In *International Conference on Learning Representations*, 2018.
- Angelina Wang and Olga Russakovsky. Directional bias amplification. In *International Conference on Machine Learning*, volume 139, pp. 10882–10893, 2021.
- Ruijia Wang, Xiao Wang, Chuan Shi, and Le Song. Uncovering the structural fairness in graph contrastive learning. In *Advances in neural information processing systems*, 2022.
- Felix Wu, Amauri Souza, Tianyi Zhang, Christopher Fifty, Tao Yu, and Kilian Weinberger. Simplifying graph convolutional networks. In *International Conference on Machine Learning*, pp. 6861–6871, 2019.
- Xinyi Wu, Zhengdao Chen, William Wang, and Ali Jadbabaie. A non-asymptotic analysis of oversmoothing in graph neural networks. In *International Conference on Learning Representations*, 2022.
- Yaochen Xie, Zhao Xu, Jingtun Zhang, Zhengyang Wang, and Shuiwang Ji. Self-supervised learning of graph neural networks: A unified review. *IEEE TPAMI*, 45(2):2412–2429, 2023.
- Wenjie Yang, Shengzhong Zhang, Jiaxing Guo, and Zengfeng Huang. Contra²: A one-step active learning method for imbalanced graphs. *Artif. Intell.*, 349:104439, 2025.
- Wenjie Yang, Shengzhong Zhang, and Zengfeng Huang. Cross-level graph contrastive learning for community value prediction. *Neural Networks*, 194:108103, 2026.
- Yuning You, Tianlong Chen, Yongduo Sui, Ting Chen, Zhangyang Wang, and Yang Shen. Graph contrastive learning with augmentations. In *Advances in neural information processing systems*, volume 33, pp. 5812–5823, 2020.
- Hengrui Zhang, Qitian Wu, Junchi Yan, David Wipf, and Philip S. Yu. From canonical correlation analysis to self-supervised graph neural networks. In *Advances in Neural Information Processing Systems*, 2021.
- Shengzhong Zhang, Zengfeng Huang, Haicang Zhou, and Ziang Zhou. SCE: scalable network embedding from sparsest cut. In *ACM SIGKDD international conference on Knowledge Discovery and Data Mining*, pp. 257–265, 2020.

Jieyu Zhao, Tianlu Wang, Mark Yatskar, Vicente Ordonez, and Kai-Wei Chang. Men also like shopping: Reducing gender bias amplification using corpus-level constraints. In *Proceedings of the 2017 Conference on Empirical Methods in Natural Language Processing*, pp. 2979–2989, 2017.

Yizhen Zheng, Shirui Pan, Vincent C. S. Lee, Yu Zheng, and Philip S. Yu. Rethinking and scaling up graph contrastive learning: An extremely efficient approach with group discrimination. In *Advances in Neural Information Processing Systems*, 2022.

Yanqiao Zhu, Yichen Xu, Feng Yu, Qiang Liu, Shu Wu, and Liang Wang. Deep graph contrastive representation learning. In *International Conference on Machine Learning Workshop on Graph Representation Learning and Beyond*, 2020.

Yanqiao Zhu, Yichen Xu, Feng Yu, Qiang Liu, Shu Wu, and Liang Wang. Graph contrastive learning with adaptive augmentation. In *Proceedings of the Web Conference*, pp. 2069–2080, 2021.

A Appendix

A.1 The proof of Lemma 4.1

Lemma A.1. *Let C_1 and C_2 be the two classes of nodes. Suppose each cluster has the same size s , then*

$$\begin{aligned} & \mathbb{E}_{P \sim \mathcal{P}} \sum_{S_i \in S} \sum_{u \in S_i} s \|f(u) - f(S_i)\|^2 \\ &= q_1 \sum_{u, v \in C_1, u \neq v} \|f(u) - f(v)\|^2 + q_2 \sum_{u, v \in C_2, u \neq v} \|f(u) - f(v)\|^2 \\ & \quad + q_{12} \sum_{u \in C_1, v \in C_2} \|f(u) - f(v)\|^2. \end{aligned}$$

Proof. Let I_u be the index such that $u \in S_{I_u}$. We have

$$\mathbb{E}_{P \sim \mathcal{P}} \sum_{S_i \in S} \sum_{u \in S_i} s \|f(u) - f(S_i)\|^2 = \mathbb{E}_{P \sim \mathcal{P}} \sum_{S_i \in S} \frac{1}{2} \sum_{u \in S_i} \sum_{v \in S_i} \|f(u) - f(v)\|^2 \quad (17)$$

For fixed $S_i \in S$, without loss of generality we assume $f(S_i) = 0$ (if not, redefine $f(u) = f(u) - f(S_i)$), then we have

$$\frac{1}{2} \sum_{u \in S_i} \sum_{v \in S_i} \|f(u) - f(v)\|^2 \quad (18)$$

$$= \frac{1}{2} \sum_{u \in S_i} \sum_{v \in S_i} (\|f(u)\|^2 + \|f(v)\|^2 - 2f(u)^T f(v)) \quad (19)$$

$$= \sum_{u \in S_i} s \|f(u) - f(S_i)\|^2. \quad (20)$$

The equation 20 is due to the assumption that $f(S_i) = 0$. Therefore,

$$\mathbb{E}_{P \sim \mathcal{P}} \sum_{S_i \in S} \sum_{u \in S_i} s \|f(u) - f(S_i)\|^2 = \mathbb{E}_{P \sim \mathcal{P}} \sum_{u \neq v} \mathbb{I}_{[I_u = I_v]} \|f(u) - f(v)\|^2. \quad (21)$$

We next divide pairs in (21) into three categories and get

$$\begin{aligned}
& \mathbb{E}_{P \sim \mathcal{P}} \sum_{u \neq v} \mathbb{I}_{[I_u=I_v]} \|f(u) - f(v)\|^2 \\
&= \mathbb{E}_{P \sim \mathcal{P}} \sum_{u, v \in C_1, u \neq v} \mathbb{I}_{[I_u=I_v]} \|f(u) - f(v)\|^2 \\
&\quad + \mathbb{E}_{P \sim \mathcal{P}} \sum_{u, v \in C_2, u \neq v} \mathbb{I}_{[I_u=I_v]} \|f(u) - f(v)\|^2 \\
&\quad + \mathbb{E}_{P \sim \mathcal{P}} \sum_{u \in C_1, v \in C_2} \mathbb{I}_{[I_u=I_v]} \|f(u) - f(v)\|^2 \\
&= \sum_{u, v \in C_1, u \neq v} q_1 \|f(u) - f(v)\|^2 + \sum_{u, v \in C_2, u \neq v} q_2 \|f(u) - f(v)\|^2 \\
&\quad + \sum_{u \in C_1, v \in C_2} q_{12} \|f(u) - f(v)\|^2,
\end{aligned}$$

which finishes the proof. \square

A.2 Comparison of Node Embeddings of the Original Graph and the Coarsened Graph

In this section, we assume the graph is connected. When there are multiple connected components, each component can be analyzed separately, and thus the conclusion holds for general graphs.

The feature matrix of the coarsened graph is computed using the formula in line 13 of Algorithm 1, which is different from prior work. Here we provide a justification on this. We consider a GNN encoder $Z = \sigma(\hat{A}^k XW)$ with $\hat{A} = \tilde{D}^{-1} \tilde{A}$. Assume the corresponding supernode of u in the coarsened graph is v . We use Z_u and Z'_v to represent the node embeddings learned from the original graph G and the coarsened graph G' respectively. We show next that using our coarsened feature matrix, the difference between Z_u and Z'_v converges to zero as $k \rightarrow \infty$.

We assume the activation function $\sigma(\cdot)$ and the linear transformation function W to be Lipschitz continuous. These assumptions are commonly used in previous analyses of GNNs (Chen et al., 2018; Garg et al., 2020; Cong et al., 2020; 2021). Then, the coarsening error can be expressed as:

$$\|Z_u - Z'_v\| = \|\sigma(\hat{A}^k XW)_u - \sigma(\hat{A}'^k X'W)_v\| \leq \kappa \|(\hat{A}^k X)_u - (\hat{A}'^k X')_v\|, \quad (22)$$

where κ represents the Lipschitz constant. For notational convenience, let $\pi_u^{(k)} = (\hat{A}^k X)_u$ and $\pi_v'^{(k)} = (\hat{A}'^k X')_v$. We need the following Lemma, the proof of which can be found in Chung & Graham (1997).

Lemma A.2.

$$\hat{A}_{i,j}^\infty = \frac{\tilde{d}_j}{\sum_{u \in G} \tilde{d}_u} = \frac{\tilde{d}_j}{2m+n}, \quad |\hat{A}_{i,j}^k - \hat{A}_{i,j}^\infty| \leq \lambda_2^k \tilde{d}_i^{-\frac{1}{2}} \tilde{d}_j^{\frac{1}{2}}, \quad (23)$$

where λ_2 is the second largest eigenvalue of \hat{A} and \tilde{d}_i denotes the degree of node i with self-loop.

Theorem A.3. Let the coarsened feature $X' = \tilde{D}'^{-1} P^T \tilde{D} X$, then for any node u , we have

$$\|\pi_u^{(k)} - \pi_v'^{(k)}\| \leq \sqrt{\frac{d_{\max}}{d_{\min}}} (n\lambda_2^k + n'\lambda_2'^k), \quad (24)$$

where λ_2 and λ_2' are the second largest eigenvalues in G and G' respectively. d_{\max} and d_{\min} are the maximum degree and minimum degree in G and G' , respectively.

Proof. Given the coarsened adjacency matrix $\tilde{A}' = P^T \tilde{A} P$, the sum of the weighted edges in \tilde{A}' is still $2m+n$. If node j in G' is not a supernode, we have $\hat{A}_{i,j}'^\infty = \frac{\tilde{d}_j}{\sum_{v \in G'} \tilde{d}_v} = \frac{\tilde{d}_j}{2m+n} = \hat{A}_{i,j}^\infty$. Let S be the set of

supernodes in G' , i.e., those nodes in G' containing at least two nodes from the original graph, and define Q as the set of nodes participating in the coarsening process: $Q = \bigcup_{S_i \in S} S_i$. Then we have:

$$\begin{aligned}
& \|\pi_u^{(k)} - \pi_v^{(k)}\| \\
&= \left\| \sum_{S_i \in S} (\hat{A}'_{v,S_i} \cdot X'_{S_i} - \sum_{j \in S_i} \hat{A}_{u,j}^k \cdot X_j) + \sum_{j \in V \setminus Q} (\hat{A}_{u,j}^k \cdot X_j - \hat{A}'_{v,j} \cdot X'_j) \right\| \\
&\leq \left\| \sum_{S_i \in S} (\hat{A}'_{v,S_i} \cdot X'_{S_i} - \sum_{j \in S_i} \hat{A}_{u,j}^k \cdot X_j) \right\| + \left\| \sum_{j \in V \setminus Q} (\hat{A}_{u,j}^k \cdot X_j - \hat{A}'_{v,j} \cdot X'_j) \right\|.
\end{aligned} \tag{25}$$

First,

$$\begin{aligned}
& \left\| \sum_{S_i \in S} (\hat{A}'_{v,S_i} \cdot X'_{S_i} - \sum_{j \in S_i} \hat{A}_{u,j}^k \cdot X_j) \right\| \\
&= \left\| \sum_{S_i \in S} (\hat{A}'_{v,S_i} \cdot X'_{S_i} - \hat{A}'_{v,S_i} \cdot X'_{S_i} + \hat{A}'_{v,S_i} \cdot X'_{S_i} \right. \\
&\quad \left. - \sum_{j \in S_i} (\hat{A}_{u,j}^k \cdot X_j - \hat{A}_{u,j}^\infty \cdot X_j + \hat{A}_{u,j}^\infty \cdot X_j)) \right\| \\
&= \left\| \sum_{S_i \in S} (\hat{A}'_{v,S_i} \cdot X'_{S_i} - \hat{A}'_{v,S_i} \cdot X'_{S_i} - \sum_{j \in S_i} (\hat{A}_{u,j}^k \cdot X_j - \hat{A}_{u,j}^\infty \cdot X_j) \right. \\
&\quad \left. + \hat{A}'_{v,S_i} \cdot X'_{S_i} - \sum_{j \in S_i} \hat{A}_{u,j}^\infty \cdot X_j) \right\| \\
&\leq \left\| \sum_{S_i \in S} (\hat{A}'_{v,S_i} \cdot X'_{S_i} - \hat{A}'_{v,S_i} \cdot X'_{S_i}) \right\| + \left\| \sum_{S_i \in S} \sum_{j \in S_i} (\hat{A}_{u,j}^k \cdot X_j - \hat{A}_{u,j}^\infty \cdot X_j) \right\| \\
&\quad + \left\| \sum_{S_i \in S} (\hat{A}'_{v,S_i} \cdot X'_{S_i} - \sum_{j \in S_i} \hat{A}_{u,j}^\infty \cdot X_j) \right\| \\
&\leq \sum_{S_i \in S} \|\hat{A}'_{v,S_i} - \hat{A}'_{v,S_i}\| \|X'_{S_i}\| + \sum_{S_i \in S} \sum_{j \in S_i} \|\hat{A}_{u,j}^k - \hat{A}_{u,j}^\infty\| \|X_j\| \\
&\quad + \left\| \sum_{S_i \in S} (\hat{A}'_{v,S_i} \cdot X'_{S_i} - \sum_{j \in S_i} \hat{A}_{u,j}^\infty \cdot X_j) \right\|.
\end{aligned} \tag{26}$$

For the sake of simplicity, we assume the feature X_j is non-negative and normalize the X_j so that $\|X_j\| = 1$.

Let the supernode feature $X'_{S_i} = \frac{\sum_{j \in S_i} \hat{A}_{u,j}^\infty X_j}{\hat{A}'_{v,S_i} \cdot \widetilde{d}_{S_i}} = \frac{\sum_{j \in S_i} \widetilde{d}_j X_j}{\sum_{j \in S_i} \widetilde{d}_j}$. In other words, the coarsened feature matrix X' is defined as $\widetilde{D}'^{-1} P^T \widetilde{D} X$, which implies $\|X'_j\| \leq 1$. Then, we have

$$\begin{aligned}
& \left\| \sum_{S_i \in S} (\hat{A}'_{v,S_i} \cdot X'_{S_i} - \sum_{j \in S_i} \hat{A}_{u,j}^k \cdot X_j) \right\| \\
&\leq \sum_{S_i \in S} \|\hat{A}'_{v,S_i} - \hat{A}'_{v,S_i}\| \|X'_{S_i}\| + \sum_{S_i \in S} \sum_{j \in S_i} \|\hat{A}_{u,j}^k - \hat{A}_{u,j}^\infty\| \|X_j\| \\
&\quad + \left\| \sum_{S_i \in S} (\hat{A}'_{v,S_i} \cdot X'_{S_i} - \sum_{j \in S_i} \hat{A}_{u,j}^\infty \cdot X_j) \right\| \\
&\leq \sum_{S_i \in S} \|\hat{A}'_{v,S_i} - \hat{A}'_{v,S_i}\| + \sum_{S_i \in S} \sum_{j \in S_i} \|\hat{A}_{u,j}^k - \hat{A}_{u,j}^\infty\| \\
&\leq \sum_{S_i \in S} \lambda'_2 \widetilde{d}_u'^{-\frac{1}{2}} \widetilde{d}_{S_i}'^{\frac{1}{2}} + \sum_{S_i \in S} \sum_{j \in S_i} \lambda_2^k \widetilde{d}_u'^{-\frac{1}{2}} \widetilde{d}_j^{\frac{1}{2}}. \quad (\text{by Lemma A.2})
\end{aligned} \tag{27}$$

For each uncoarsened node $u \in V \setminus Q$, we have $\hat{A}_{u,j}^\infty = \hat{A}'_{v,j}$ and $X_j = X'_j$. Therefore,

$$\begin{aligned}
& \left\| \sum_{j \in V \setminus Q} (\hat{A}_{u,j}^k \cdot X_j - \hat{A}'_{v,j} \cdot X'_j) \right\| \\
&= \left\| \sum_{j \in V \setminus Q} (\hat{A}_{u,j}^k \cdot X_j - \hat{A}_{u,j}^\infty \cdot X_j + \hat{A}_{u,j}^\infty \cdot X_j - \hat{A}'_{v,j} \cdot X'_j) \right\| \\
&\leq \sum_{j \in V \setminus Q} (\|\hat{A}_{u,j}^k \cdot X_j - \hat{A}_{u,j}^\infty \cdot X_j\| + \|\hat{A}_{u,j}^\infty \cdot X_j - \hat{A}'_{v,j} \cdot X'_j\|) \\
&\leq \sum_{j \in V \setminus Q} (\|\hat{A}_{u,j}^k - \hat{A}_{u,j}^\infty\| + \|\hat{A}'_{v,j} - \hat{A}_{v,j}^\infty\|) \\
&\leq \sum_{j \in V \setminus Q} (\lambda_2^k \tilde{d}_u^{-\frac{1}{2}} \tilde{d}_j^{\frac{1}{2}} + \lambda_2'^k \tilde{d}_v^{-\frac{1}{2}} \tilde{d}_j^{\frac{1}{2}}). \quad (\text{by Lemma A.2})
\end{aligned} \tag{28}$$

We define d_{max} and d_{min} as the maximum degree and minimum degree in G and G' , respectively. Thus, we have the following conclusion

$$\begin{aligned}
& \|\pi_u^{(k)} - \pi_v'^{(k)}\| \\
&\leq \sqrt{\frac{d_{max}}{d_{min}}} |S| \lambda_2'^k + \sqrt{\frac{d_{max}}{d_{min}}} |Q| \lambda_2^k + \sqrt{\frac{d_{max}}{d_{min}}} (n - |Q|) (\lambda_2^k + \lambda_2'^k) \\
&= \sqrt{\frac{d_{max}}{d_{min}}} (n \lambda_2^k + (n + |S| - |Q|) \lambda_2'^k) \\
&= \sqrt{\frac{d_{max}}{d_{min}}} (n \lambda_2^k + n' \lambda_2'^k).
\end{aligned} \tag{29}$$

□

According to Theorem A.3 and inequality (22), we have the following upper bound:

$$\|Z_u - Z_v'\| \leq \kappa \sqrt{\frac{d_{max}}{d_{min}}} (n \lambda_2^k + n' \lambda_2'^k). \tag{30}$$

On the account of $0 < \lambda_2 < 1$ and $0 < \lambda_2' < 1$, when $k \rightarrow \infty$, the error $\|Z_u - Z_v'\| \rightarrow 0$.

A.3 Generalizability of RGCCL

Following (Huang et al., 2023; Wang et al., 2022), we investigate the generalizability of our self-supervised model. Denote \mathcal{G}_{v_i} as the ego network of node v_i and the corresponding adjacency matrix as $\hat{A}_{\mathcal{G}_{v_i}}$, Wang et al. (2022) characterizes the concentration of a graph augmentation set with the following definition.

Definition 2 ($(\alpha, \gamma, \hat{d})$ -Augmentation). *The data augmentation set A , which includes the original graph, is a $(\alpha, \gamma, \hat{d})$ -augmentation, if for each class C_k , there exists a main part $C_k^0 \subseteq C_k$ (i.e., $\mathbb{P}[v \in C_k^0] \geq \sigma \mathbb{P}[v \in C_k]$), where $\sup_{v_1, v_2 \in C_k^0} d_A(v_1, v_2) \leq \gamma (\frac{\mathcal{D}}{\hat{d}_{min}^k})^{1/2}$ hold with $d_A(v_i, v_j) = \min_{\mathcal{G}'_i \in A(\mathcal{G}_{v_i}), \mathcal{G}'_j \in A(\mathcal{G}_{v_j})} \|(\frac{\hat{A}_{\mathcal{G}'_i}}{\hat{d}_{\mathcal{G}'_i}} - \frac{\hat{A}_{\mathcal{G}'_j}}{\hat{d}_{\mathcal{G}'_j}})X\|$, and \hat{d}_{min}^k is the minimum degree in class C_k .*

Given a $(\alpha, \gamma, \hat{d})$ -Augmentation, one can establish inequalities between contrastive losses and the dot product of class center pairs. This means classes will be more separable while the objectives are being optimized. For example, Huang et al. (2023) gives the proofs for InfoNCE and the cross-correlation loss. Since our objective differs from both of them, we prove a similar theorem as Huang et al. (2023). Denote $\mu_k := \mathbb{E}_{v \in C_k} \mathbb{E}_{\mathcal{G}' \in A(\mathcal{G}_v)} [f(\mathcal{G}')]$, $p_k := \mathbb{P}[v \in C_k]$, $S_\epsilon := \{v \in \bigcup_{k=1}^K C_k : \forall \mathcal{G}_1, \mathcal{G}_2 \in A(\mathcal{G}_v), \|f(\mathcal{G}_1) - f(\mathcal{G}_2)\| \leq \epsilon\}$ and $R_\epsilon := 1 - \mathbb{P}[S_\epsilon]$.

Theorem A.4. Assume that encoder f with norm 1 is M -Lipschitz continuous. For a given $(\alpha, \gamma, \hat{d})$ augmentation set A , any $\epsilon > 0$ and $k \neq l$,

$$\mu_k^T \mu_l \leq \frac{1}{p_k p_l} \left(-\frac{1}{2n^2 \mathcal{L}_{neg}} + \tau(\epsilon, \alpha, \gamma, \hat{d}) \right), \quad (31)$$

where $\tau(\epsilon, \alpha, \gamma, \hat{d}) = 2R_\epsilon + 16(1 - \alpha(1 - \frac{1}{2}\epsilon - \frac{1}{4}M \max_k(\gamma \sqrt{\frac{\mathcal{D}}{d_{\min}^k}})) + KR_\epsilon)^2 + 8(1 - \alpha(1 - \frac{1}{2}\epsilon - \frac{1}{4}M \max_k(\gamma \sqrt{\frac{\mathcal{D}}{d_{\min}^k}})) + KR_\epsilon + \frac{K-1}{K})$.

Proof. Our negative pair loss is

$$\begin{aligned} \mathcal{L}_{neg} &= \mathbb{E}_{P \sim \mathcal{P}} \left[\frac{1}{\sum_{i=1}^n \sum_{j=1}^n [\|h_i\|^2 + \|h_j\|^2 - 2h_i^T h_j]} \right] \\ &= \frac{1}{2} \mathbb{E}_{P \sim \mathcal{P}} \left[\frac{1}{n^2 - \sum_{i=1}^n \sum_{j=1}^n h_i^T h_j} \right]. \end{aligned}$$

Since $\sum_{i=1}^n \sum_{j=1}^n h_i^T h_j \leq n^2$, and $\frac{1}{n^2 - x}$ is convex for $x \leq n^2$. Using Jensen's inequality, we have:

$$\begin{aligned} 2\mathcal{L}_{neg} &\geq \frac{1}{n^2 - \mathbb{E}_{P \sim \mathcal{P}} [\sum_{i=1}^n \sum_{j=1}^n h_i^T h_j]} \\ &= \frac{1}{n^2 (1 - \mathbb{E}_{x_i, x_j} \mathbb{E}_{P \sim \mathcal{P}} [h_i^T h_j])}. \end{aligned}$$

Next, we focus on $\mathbb{E}_{x_i, x_j} \mathbb{E}_{P \sim \mathcal{P}} h_i^T h_j$:

$$\begin{aligned} \mathbb{E}_{x_i, x_j} \mathbb{E}_{P \sim \mathcal{P}} [h_i^T h_j] &\geq \sum_{k=1}^K \sum_{l=1}^K \mathbb{E}_{x_i, x_j} [\mathbb{I}(x_i \in S_\epsilon \cap C_k) \mathbb{I}(x_j \in C_l) \mathbb{E}_{P \sim \mathcal{P}} (h_i^T h_j)] \\ &\quad - \mathbb{E}_{x_i, x_j} [\mathbb{I}(x_i \in \bar{S}_\epsilon)] \\ &= \sum_{k=1}^K \sum_{l=1}^K \mathbb{E}_{x_i, x_j} [\mathbb{I}(x_i \in C_k) \mathbb{I}(x_j \in C_l) (\mu_k^T \mu_l)] - R_\epsilon + \Delta_1 \\ &= \sum_{k=1}^K \sum_{l=1}^K [p_k p_l \mu_k^T \mu_l] - R_\epsilon + \Delta_1 \\ &\geq p_k p_l \mu_k^T \mu_l + \frac{1}{K} - R_\epsilon + \Delta_1, \end{aligned}$$

where Δ_1 is defined as

$$\begin{aligned} \Delta_1 &= \sum_{k=1}^K \sum_{l=1}^K \mathbb{E}_{x_i, x_j} [\mathbb{I}(x_i \in S_\epsilon \cap C_k) \mathbb{I}(x_j \in C_l) \mathbb{E}_{P \sim \mathcal{P}} (h_i^T h_j)] \\ &\quad - \sum_{k=1}^K \sum_{l=1}^K \mathbb{E}_{x_i, x_j} [\mathbb{I}(x_i \in C_k) \mathbb{I}(x_j \in C_l) (\mu_k^T \mu_l)] \\ &= \sum_{k=1}^K \sum_{l=1}^K \mathbb{E}_{x_i, x_j} [\mathbb{I}(x_i \in C_k) \mathbb{I}(x_j \in C_l) \mathbb{E}_{P \sim \mathcal{P}} [h_i^T h_j - \mu_k^T \mu_l]] \\ &\quad - \sum_{k=1}^K \sum_{l=1}^K \mathbb{E}_{x_i, x_j} [(\mathbb{I}(x_i \in C_k) - \mathbb{I}(x_i \in S_\epsilon \cap C_k)) \mathbb{I}(x_j \in C_l) \mathbb{E}_{P \sim \mathcal{P}} (h_i^T h_j)]. \end{aligned}$$

Then,

$$\begin{aligned}
|\Delta_1| &\leq R_\epsilon + \sum_{k=1}^K \sum_{l=1}^K \mathbb{E}_{x_i, x_j} [\mathbb{I}(x_i \in C_k) \mathbb{I}(x_j \in C_l) \mathbb{E}_{P \sim \mathcal{P}} |h_i^T h_j - \mu_k^T \mu_l|] \\
&\leq R_\epsilon + 16(1 - \alpha(1 - \frac{1}{2}\epsilon - \frac{1}{4}M\max_k(\gamma\sqrt{\frac{\mathcal{D}}{\hat{d}_{\min}^k}})) + KR_\epsilon)^2 \\
&\quad + 8(1 - \alpha(1 - \frac{1}{2}\epsilon - \frac{1}{4}M\max_k(\gamma\sqrt{\frac{\mathcal{D}}{\hat{d}_{\min}^k}})) + KR_\epsilon).
\end{aligned}$$

Thus, if we define

$$\begin{aligned}
\tau(\epsilon, \alpha, \gamma, \hat{d}) &= 2R_\epsilon + 16(1 - \alpha(1 - \frac{1}{2}\epsilon - \frac{1}{4}M\max_k(\gamma\sqrt{\frac{\mathcal{D}}{\hat{d}_{\min}^k}})) + KR_\epsilon)^2 \\
&\quad + 8(1 - \alpha(1 - \frac{1}{2}\epsilon - \frac{1}{4}M\max_k(\gamma\sqrt{\frac{\mathcal{D}}{\hat{d}_{\min}^k}})) + KR_\epsilon + \frac{K-1}{K}),
\end{aligned}$$

we have

$$\begin{aligned}
\mu_k^T \mu_l &\leq \frac{1}{p_k p_l} (1 - \frac{1}{2n^2 \mathcal{L}_{neg}} - \frac{1}{K} + R_\epsilon + |\Delta_1|) \\
&\leq \frac{1}{p_k p_l} (-\frac{1}{2n^2 \mathcal{L}_{neg}} + \tau(\epsilon, \alpha, \gamma, \hat{d})).
\end{aligned}$$

This finishes the proof. \square

A.4 Random Graph Coarsening Algorithm

Algorithm 1 is a detailed description of our random graph coarsening algorithm.

Algorithm 1 Random Graph Coarsening

Input: $G = (A, X)$, threshold δ , the coarsening ratio r , number of nodes n

Output: $G' = (A', X')$

Compute the weight set \mathcal{I} of all edges

Construct an edge set \mathcal{E} of length rn by randomly selecting the edges according to the weight set \mathcal{I} .

Initialize the cluster list \mathcal{T}

for $i = 0$ to rn **do**

Obtain $(u, v) = \mathcal{E}_i$

Retrieve the clusters \mathcal{T}_u and \mathcal{T}_v from \mathcal{T} , where \mathcal{T}_u contains u and \mathcal{T}_v contains v

if $|\mathcal{T}_u| + |\mathcal{T}_v| < \delta$ and $\mathcal{T}_u \neq \mathcal{T}_v$ **then**

Merge cluster \mathcal{T}_u and cluster \mathcal{T}_v to a new cluster

end if

end for

Construct the assignment matrix P by \mathcal{T}

Compute the coarsened adjacency matrix $A' = P^T A P$

Compute the coarsened feature matrix $X' = \tilde{D}'^{-1} P^T \tilde{D} X$

Return $G' = (A', X')$

A.5 Experimental details

For all unsupervised models, the learned representations are evaluated by training and testing a logistic regression classifier except for Ogbn-Arxiv. Since Ogbn-arxiv exhibits more complex characteristics, we use a more powerful MLP classifier. The detailed statistics of the six datasets are summarized in Table 7.

Table 7: Summary of the datasets used in our experiments

Dataset	Nodes	Features	Classes	Avg. Degree
Cora	2,708	1,433	7	3.907
Citeseer	3,327	3,703	6	2.74
Pubmed	19,717	500	3	4.50
Amazon-Photo	7,650	745	8	31.13
Amazon-Computers	13,752	767	10	35.76
Ogbn-Arxiv	169,343	128	40	13.67

Details of our model. In our model, we use SGC as the encoder for Cora, Citeseer, Pubmed, while we use GCN as the encoder for Photo and Computers. The detailed hyperparameter settings are listed in Table 8. Our code is available at: <https://github.com/szzhang17/Understanding-Class-Bias-Amplification-in-Graph-Representation-Learning>.

Table 8: Summary of the hyper-parameters.

Dataset	Epoch	Learning rate	α	β
Cora	25	0.01	15000	500
Citeseer	200	0.0002	15000	500
Pubmed	25	0.02	20000	200
Amazon-Photo	20	0.001	100000	100000
Amazon-Computers	20	0.0002	20000	20000
Ogbn-Arxiv	10	0.0001	2000000	200000

Details of Baselines. We compare RGCCL with state-of-the-art GCL models DGI¹, GRACE², GraphCL³, GCA⁴, CCA-SSG⁵, gCooL⁶, GGD⁷, GRADE⁸, SPAN⁹, PolyGCL¹⁰ and classic graph embedding model Deepwalk. For all the baseline models, we use the source code from corresponding repositories. Due to the large scale of Ogbn-Arxiv, some GCL models are unable to process the full-graph on GPU because of memory limitations. As a result, we apply graph sampling techniques to train these models.

Configuration. All the algorithms and models are implemented in Python and PyTorch Geometric. Experiments are conducted on a server with NVIDIA 3090 GPU (24 GB memory), NVIDIA A6000 GPU (48 GB memory) and Intel(R) Xeon(R) Silver 4210R CPU @ 2.40GHz.

¹DGI (MIT License): https://github.com/pyg-team/pytorch_geometric/blob/master/examples/infomax_transductive.py

²GRACE (Apache License 2.0): <https://github.com/CRIPAC-DIG/GRACE>

³GraphCL (MIT License): <https://github.com/Shen-Lab/GraphCL>

⁴GCA (MIT License): <https://github.com/CRIPAC-DIG/GCA>

⁵CCA-SSG (Apache License 2.0): <https://github.com/hengruizhang98/CCA-SSG>

⁶gCooL (MIT License): <https://github.com/lblaoke/gCooL>

⁷GGD (MIT License): <https://github.com/zyzisastudyreallyhardguy/Graph-Group-Discrimination>

⁸GRADE (MIT License): <https://github.com/BUPT-GAMMA/Uncovering-the-Structural-Fairness-in-Graph-Contrastive-Learning>

⁹SPAN (MIT License): <https://github.com/Louise-LuLin/GCL-SPAN>

¹⁰PolyGCL (MIT License): <https://github.com/ChenJY-Count/PolyGCL>